Contemporary Mathematics
http://ojs.wiserpub.com/index.php/CM/

Research Article

Analytical Study of (2 + 1)-Dimensional Time Fractional Bogoyavlensky-Konopelchenko Model in Plasma and Fluid Dynamics

Saleh Alshammari[1], M. Mossa Al-sawalha[1], Mohammad Alshammari[1], Yousef Jawarneh[1], Mohammed Al-Smadi[2,3], Mohammed Alabedalhadi[2*]

[1] Department of Mathematics, College of Science, University of Ha'il, Ha'il 2440, Saudi Arabia
[2] Department of Applied Science, Ajloun College, Al-Balqa Applied University, Ajloun 26816, Jordan
[3] College of Commerce and Business, Lusail University, Lusail, Qatar
E-mail: mohmdnh@bau.edu.jo

Received: 17 November 2025; **Revised:** 16 March 2026; **Accepted:** 10 April 2026

Abstract: This paper studies the (2 + 1)-dimensional time fractional Bogoyavlensky-Konopelchenko model that is significant in plasma physics and fluid dynamics. We enhance the model with the Caputo fractional derivative to account for memory and hereditary qualities present in complex physical systems. We use a method called the Laplace residual power series approach to find approximate solutions for the governing model. This approach combines the residual power series technique and the Laplace transform to obtain approximate solutions that represent the dynamic behavior of the governing system. Analytical solutions are derived using the proposed approach, and the exact solutions of the system are compared with those explored during the work, and the absolute and relative errors in the classical case are determined. A comparison of the dynamic behavior of the system at different orders of fractional derivatives and the effect of changing order on the behavior of the derived solutions is presented. To connect the numerical results with physical interpretations, physical insights based on the derived solutions are presented by studying the energy evolution in two different cases of initial conditions. This study advances mathematical models for complicated physical processes, paving the way for practical applications in engineering and science.

Keywords: fractional differential equations, residual power series method, plasma physics, fluid dynamics

MSC: 34A08, 35R11

1. Introduction

The Bogoyavlensky-Konoplechenko (BK) model is an important mathematical model for understanding nonlinear processes in many fields, such as nonlinear optics, fluid dynamics, and plasma physics [1]. The importance of the model lies in its ability to explain the motion of waves in a two-dimensional space, which improves its ability to explain the propagation of waves through many complex physical systems [2]. The model is used to detect the actions of light in photosensitive systems and optical paths, which expresses its importance in the context of nonlinear optics [3]. In the field of fluid dynamics, the model is used to explain the transmission of nonlinear waves such as surface waves and gas waves in liquids [4]. In addition, the model is employed to study the importance of waves in plasmas and explain their

DOI: https://doi.org/10.37256/cm.7420269176

effect on both the electrical and magnetic properties of space [5]. The model originated in the 1970s when Bogoevlensky and Konoplechenko formulated it as a comprehensive framework that extends the Korteweg-de Vries (KdV) equation, which depicted one-dimensional wave interactions, to include several temporal and spatial dimensions [6]. Subsequently, the model has been augmented to include nonlinear effects across many dimensions and has been used in other scientific disciplines, establishing it as a crucial instrument for comprehending intricate dynamical systems [7]. Currently, the model is integral to mathematical physics and applied mathematics, utilized for analyzing stability, traveling wave solutions, and complex impulses in kinetic systems, thereby aiding the advancement of technological solutions in fields like optical processing and wave control [8].

The BK model in its fractional form is a powerful and important tool in analyzing complex dynamic systems considering nonlinear interactions and memory effects [9]. The fractional derivative is used instead of the ordinary derivative, which allows the model in its fractional form to interpret the effect of time or space in a non-local manner, which means that the interactions in the system do not depend only on the current state, but rather the interactions depend on previous states of the system, which gives the fractional system a great ability to represent natural phenomena more accurately than the traditional model, such as continuous energy conservation and processes that include memory [10]. The ordinary derivative is limited to describing linear changes within the system and cannot analyze the historical or distant effects of past conditions, in contrast to the fractional derivative, which can analyze these phenomena more precisely. In plasma physics, the fractional derivative describes the effect of non-local interactions in the plasma, including the propagation of waves affected by past conditions [11]. As for the importance of the fractional derivative in fluid dynamics, the fractional derivative is used to explain the propagation of surface waves in the oceans or in complex hydrodynamic systems that have memory-based behavior [12]. In addition, the importance of the fractional model in the field of nonlinear optics lies in its use to study the propagation of optical waves in optical fibers with a repetitive effect [13]. Moreover, the fractional model has a major role in the field of biological systems, where it is used to study the effect of time on interactions between tissues and cells [14]. In this paper, we study the following (2 + 1)-dimensional time fractional BK equation:

$$\begin{aligned}&\mathscr{D}_t^{\beta} w_x(t,x,y)+\mu_1 w_{xxxx}(t,x,y)+\mu_2 w_{xxxy}(t,x,y)+6\mu_1 w_{xx}(t,x,y)w_x(t,x,y)\\&+4\mu_2 w_{xy}(t,x,y)w_x(t,x,y)+4\mu_2 w_{xx}(t,x,y)w_y(t,x,y)=0.\end{aligned} \tag{1}$$

The symbole $\mathscr{D}_t^{\beta}$ denotes the Caputo fractional derivative of order β with repect to the temporal t. The function $w(t,x,y)$ represents the state function of the spatial variavles x, y and the temporal variable t. The term $w_x(t,x,y)$ is the the spatial change in the direction of x. The term $\mu_1 w_{xxxx}(t,x,y)$ denotes a fourth-order spatial diffusion impact on w in the x-direction, scaled by μ_1. The term $\mu_2 w_{xxxy}(t,x,y)$ represents mixed spatial interactions between the derivatives in both the x and y directions, scaled by μ_2. The terms $w_{xx}w_x$, $w_{xy}w_x$ and $w_{xx}w_y$ stand for nonlinearity. The parameter μ_1 represents the scattering strength along the x-direction, while μ_2 represents the mixed scattering coupling between the spatial variables x and y. The relationship between the two parameters can be described by the ratio μ_2/μ_1 , which defines the anisotropy of the dispersed medium's properties. This equation (1) studies the interaction of a Riemann wave moving along the y-axis accompanied by a long wave along the x-axis in a fluid. It is of great importance in fluid dynamics as it enables research into how waves traveling in different directions affect the medium, which helps researchers study acoustic waves in the oceans or atmosphere. In addition to its important role in developing control techniques in liquid systems. Equation (1) can be classified as an evolutionary partial differential equation that combines two- and fourth-order dispersion terms, placing it within the hierarchy of generalizations of the KdV equation to two spatial dimensions. The significance of this (2 + 1)-dimensional governing equation lies in its rich hierarchical structure, where it connects complex nonlinear interactions with high-order dispersion terms, unlike its counterparts, which are often integrable extensions of one-dimensional equations. This property of the equation makes it a powerful tool for modeling complex wave phenomena where nonlinear energy transfer and dispersion are strong, phenomena common in the contexts of plasma physics and fluid dynamics. In plasma context, the fractional derivative shows how groups of particles that are trapped together affect how waves move. In kinds of plasmas that have a magnetic field some particles get stuck in the valleys of waves that have a certain size and they move around in a regular path that remembers where they started. These trapped particles do not change what they are doing away when the field around them changes. Instead, how they affect the properties of the plasma depends on everything that has happened to them. The fractional derivative order β decides how many particles are trapped compared to how many're moving freely. When β is close, to one it means the plasma is mostly made up of particles that are moving freely. When β gets smaller it means there are more trapped particles that remember things for a longer time. This causes waves and particles to interact in ways and makes things relax slowly. In In fluid dynamics, the fractional derivative is really good at showing how complex fluids remember what happened to them. This is important for things like solutions, emulsions or turbulent flows. The stress on these fluids at any point does not just depend on what's happening to them right now but also on what happened to them in the past. The fractional derivative order, which is called β controls how quickly the fluid forgets what happened to it. When β is 1 the fluid is like a fluid it does not remember anything. When β is less than 1 the fluid starts to act like it has a memory and this memory is what makes it viscoelastic. The way the stress on the fluid decreases, over time follows some rules that scientists have seen when they study fluids.

Researchers have addressed the BK equation in many studies. In [15], the authors introduced a new approach to investigating nonlinear evolution equations with variable coefficients and applied it to the BK equation. In [16], the authors utilized the Hirota bilinear approaches to explore explicit lump solutions for the BK equation. In [17], the conservation laws for the (2 + 1)-dimensional BK equation are obtained using the new conservation theorem method and the formal Lagrangian approach. Exact solutions for the BK model have been obtained using the $\left(\frac{G'}{G^2}\right)$-method in [18]. Symmetry solutions for the BK equation have been constructed using three distinct approaches in [19]. In [20], the authors used the semi-inverse variational principle to gain localized waves, including soliton, periodic, and cross-kink solutions for the BK model. Ismael et al constructed multi-soliton and one-M-lump solutions for the BK model and presented a dynamical study and physical behaviors of the resulting solutions [21]. Ali et al. obtained solitary solutions using Lie symmetry analysis for the BK model [22]. In our work, we seek to utilize the Laplace Residual Power Series (LRPS) method to expose analytical solutions for the (2 + 1)-dimensional time fractional BK equation (1). The significance of the transition from classical to fractional dynamics for the governing model lies in incorporating memory effects. This enables us to study complex long-range interactions and identify heredity properties that are not addressed within the classical framework, which in turn leads to more accurate modeling of complex physical phenomena. To our knowledge, numerical solutions of the governing model (1) have been presented in [10] only, where the authors used the conformable definition to describe the fractional derivative. This leads us to study the fractional governing model in the context of Caputo's definition, which relies on the complete history of $w(t, x, y)$ from 0 to t, while the conformable derivative relies on the behavior of the function $w(t, x, y)$ in the vicinity of point t. This makes Caputo's definition more suitable for modeling physical phenomena such as wave propagation in fluids and plasmas. Furthermore, the initial conditions in Caputo's definition have a clear physical meaning. This motivates us to present this study in which we use Caputo's definition to describe the fractional derivative and exploit the proposed method to create novel numerical solutions for the governing equation. We also look forward to studying the effects of the fractional derivative on the behavior of the explored solutions and providing physical explanations for these effects. We also seek to study the effect of changing the values of the parameters on the results.

We organize the paper as follows: introduction, Section 2 is devoted to presenting the preliminaries and the proposed approach. In Section 3, we apply to the LRPS method to obtain numerical solutions for the (2 + 1)-dimensional time fractional BK equation (1). Section 4 is devoted to introducing numerical simulations for the results obtained in Section 3. Some physical applications are presented in Section 5. Some conclusions and future recommendations are presented in Section 6.

2. Preliminary

2.1 *Fractional calculus*

Fractional derivatives have various definitions, each with advantages and uses of their own. In our work, we consider the Caputo fractional derivative.

Definition 1 [23] For an integrable function ψ, the Caputo derivative of fractional order $\beta \in (0,1)$ is given by:

$$\mathscr{D}_t^{\beta} w(t) = \frac{1}{\Gamma(h-\beta)} \int_0^t \frac{\partial^h w(t)}{\partial t^h} \frac{1}{(t-\tau)^{\beta-h+1}} d\tau, \tag{2}$$

where $t \geq 0,\ h = [\beta]+1$. The Riemann-Liouville fractional integral of order $\beta,\ Re(\beta) > 0$ is given by:

$$\mathscr{I}_t^{\beta} w(t) = \frac{1}{\Gamma(\beta)} \int_0^t (t-\tau)^{\beta-1} w(\tau) d\tau. \tag{3}$$

Lemma 1 [23] For $0 < \beta < 1$ and $t \geq 0$, we get the following property for Caputo derivative:

$$\mathscr{I}_t^{\beta} \mathscr{D}_t^{\beta} w(t) = w(t) - \sum_{k=0}^{h-1} \frac{d^k w(0)}{dt^i} \frac{t^k}{k!}. \tag{4}$$

Definition 2 [23] Let $w(t)$ be a piecewise continuous function on $[0,\infty)$ and of exponential order σ. The Laplace Transformation (LT) of $w(t)$ is defined as:

$$\mathscr{W}(s) = \mathfrak{L}\{w(t)\} = \int_0^{\infty} e^{-st} w(t) dt,\ s > \sigma, \tag{5}$$

while the inverse Laplace transformation of $\mathscr{W}(s,x)$ is given by:

$$w(t) = \mathfrak{L}^{-1}\{\mathscr{W}(s)\} = \int_{v-i\infty}^{v+i\infty} e^{st} \mathscr{W}(s) ds,\ v = Re(s) > v_0, \tag{6}$$

where v_0 lies in the right half plane of the absolute convergence of the Laplace integral.

Lemma 2 [24] Let $w(t)$ be piecewise continuous function on $[0,\infty)$ and of exponential order σ, and $\mathscr{W}(s) = \mathfrak{L}\{w(t)\}$. Then:

1. $\lim_{s\to\infty} s\mathscr{W}(s) = w(0)$.
2. $\mathfrak{L}\left\{\mathscr{I}_t^{\beta} w(t)\right\} = \frac{\mathscr{W}(s)}{s^{\beta}},\ \beta > 0$.
3. $\mathfrak{L}\left\{\mathscr{D}_t^{\beta} w(t)\right\} = s^{\beta}\mathscr{W}(s) - \sum_{k=0}^{h-1} s^{\beta-k-1} \frac{d^k w(0)}{dt^k}$.

2.2 *Laplace residual power series method*

Fractional differential equations require special methods so that we can derive and extract exact or numerical solutions due to the complexities we face when considering fractional derivatives in the systems being studied [25–27]. This urgent need prompted scientists and researchers to provide and develop effective and appropriate methods to reach the desired solutions. For instance, the finite difference approaches [28], multistep approach [29], Riccati-Bernoulli sub-ODE method [30], the generalized Taylor's formula [31], multistep generalized differential transform method [32], Fractional residual series method [33], homotopy analysis method [34], Jacobi Polynomials approach [35], and Legendre polynomials approach [36]. The LRPS technique is a mathematical strategy for solving fractional differential equations [37]. It offers a disciplined approach to solving equations with fractional derivatives analytically. The method involves solving the original equation in the time domain by applying inverse Laplace transforms after translating it into the Laplace domain, expressing it as a power series, and analyzing the residual series. It is a crucial tool in fields such as applied mathematics, engineering, and physics because it is particularly useful when traditional analytical methods fail to solve difficult fractional calculus problems [38–41].

Theorem 1 [42] Let $w(t)$ be piecewise continuous function on $[0,\infty)$ and of exponential order σ, and $\mathscr{W}(s)=\mathfrak{L}\{w(t)\}$. Then the transformed function $\mathscr{W}(s)$ can be represented in the following expansion:

$$\mathscr{W}(s)=\sum_{p=0}^{\infty}\frac{A_p}{s^{1+p\beta}},\ 0<\beta\leq 1,\ s>\sigma, \tag{7}$$

where the coefficients $A_p=\mathscr{D}_t^{p\beta}w(0),\ p=0,1,2,\ldots$. Moreover, the inverse Laplace transformation of the expansion (7) can be given as:

$$w(t)=\sum_{p=0}^{\infty}\frac{\mathscr{D}_t^{p\beta}w(0)}{\Gamma(p\beta+1)}t^{p\beta}. \tag{8}$$

Furthermore, if $\left|s\mathfrak{L}\left\{\mathscr{D}_t^{(p+1)\beta}w(t)\right\}\right|<\mathfrak{M}$ on $0<s\leq d$ where $0<\beta\leq 1$, then the remainder $\mathfrak{R}_p(s)$ of the expression (8) satisfies the following:

$$|\mathfrak{R}_p(s)|\leq\frac{\mathfrak{M}}{s^{(p+1)\beta+1}},\ 0<s\leq d. \tag{9}$$

Theorem 1 explains and determines the conditions for convergence of Taylor's formula (7). Now, we present the algorithm for the LRPS method of Nonlinear Fractional Differential Equation (NFDE).

Algorithm. LRPS method for the NFDE

Step I. Consider the following NFDE:

$$\mathscr{D}_t^{\beta}w(t)-\mathfrak{N}(w(t))-f(t)=0, \tag{10}$$

subject to the initial condition:

$$w(0)=w_0, \tag{11}$$

where $\mathscr{D}_t^{\beta}$ is the Caputo derivative of order β; $(0<\beta<1)$ with respect to t, $\mathfrak{N}$ are well-known nonlinear analytical functions.

Step II. Applying LT to both sides of (10) with aid of Lemma 2 to get:

$$\mathscr{W}(s)-\frac{1}{s}w_0-\frac{1}{s^{\beta}}\mathfrak{N}_L(s)-\frac{1}{s^{\beta}}\mathscr{F}(s)=0, \tag{12}$$

where$\mathscr{W}(s) = \mathfrak{L}\{w(t)\}$, $\mathfrak{N}_L(s) = \mathfrak{L}\{\mathfrak{N}(w(t))\}$ and $\mathscr{F}(s) = \mathscr{L}\{f(t)\}$.

Step III. The solutions of equation (12) assumed to be in the form:

$$\mathscr{W}(s) = \sum_{p=0}^{\infty} \frac{A_p}{s^{p\beta+1}},\ s > 0, \tag{13}$$

where A_p are coefficients to be determined. Using part (1) in Lemma 2 to obtain the initial coefficient in the series (13) as: $A_0 = w_0$. Hence, the solutions of system (12) can be written as:

$$\mathscr{W}(s) = \frac{w_0}{s} + \sum_{p=1}^{\infty} \frac{A_p}{s^{p\beta+1}},\ s > 0. \tag{14}$$

Step IV. Define the Nth-truncated series of $\mathscr{W}(s)$ in the form:

$$\mathscr{W}^N(s) = \frac{w_0}{s} + \sum_{p=1}^{N} \frac{A_p}{s^{p\beta+1}},\ s > 0. \tag{15}$$

Step V. Define the Laplace residual function:

$$\mathfrak{L}\mathfrak{R}es(s) = \mathscr{W}(s) - \frac{w_0}{s} - \frac{1}{s^\beta}\mathfrak{N}_L(s) - \frac{1}{s^\beta}\mathscr{F}(s), \tag{16}$$

where $\mathscr{W}(s)$ as in (14). In addition, we define the Nth-Laplace residual function as follows:

$$\mathfrak{L}\mathfrak{R}es^N(s) = \mathscr{W}^N(s) - \frac{w_0}{s} - \frac{1}{s^\beta}\mathfrak{N}_L(s) - \frac{1}{s^\beta}\mathscr{F}(s), \tag{17}$$

where $\mathscr{W}^N(s)$ as in (15).

Step VI. Multiply (17) by $s^{p\beta+1},\ p = 1, 2, \dots N$, then solve the obtained algebraic equations:

$$\lim_{s\to\infty} s^{p\beta+1}\mathfrak{L}\mathfrak{R}es^p(s) = 0, \tag{18}$$

to determine the coefficients $A_1,\ A_2, \dots, A_N$, respectively.

Step VII. Substitute the inferred coefficients $A_p, p = 1, 2, \dots, N$, in (15) to obtain the Nth solutions for $\mathscr{W}(s)$.

Step VIII. Apply the inverse LT to obtained $\mathscr{W}(s)$ in Step 7, with using Theorem 1 to obtain the Nth LRPS solutions $w(t)$ for the NFDE (17) in the form:

$$w^N(t) = w_0 + \sum_{p=1}^{N} \frac{A_p}{\Gamma(p\beta+1)} t^{p\beta}. \tag{19}$$

3. Application of LRPS method for the (2 + 1)-dimensional time fractional BK equation

Herein, we utilize the proposed algorithm to obtain numerical solution for the (2 + 1)-dimensional time fractional BK equation (1) with the following initial condition:

$$w(0,x,y) = w_0(x,y). \tag{20}$$

Firstly, we apply for the LT for both sides of (1) to get:

$$\begin{aligned} &\mathfrak{L}\left\{\mathscr{D}_t^{\beta} w_x(t,x,y)\right\} + \mu_1 \mathfrak{L}\{w_{xxxx}(t,x,y)\} + \mu_2 \mathfrak{L}\{w_{xxxy}(t,x,y)\} + 6\mu_1 \mathfrak{L}\{w_{xx}(t,x,y)w_x(t,x,y)\} \\ &+ 4\mu_2 \mathfrak{L}\{w_{xy}(t,x,y)w_x(t,x,y)\} + 4\mu_2 \mathfrak{L}\{w_{xx}(t,x,y)w_y(t,x,y)\} = 0, \end{aligned} \tag{21}$$

Using Lemma 2 we get:

$$\begin{aligned} \mathfrak{L}\left\{\mathscr{D}_t^{\beta} w_x(t,x,y)\right\} &= s^{\beta} \mathfrak{L}\{w_x(t,x,y)\} - s^{\beta-1}\frac{\partial}{\partial x} w_0(x,y) \\ &= s^{\beta}\frac{\partial}{\partial x}\mathscr{W}(s,x,y) - s^{\beta-1}\frac{\partial}{\partial x} w_0(x,y), \end{aligned} \tag{22}$$

where $\mathscr{W}(s,x,y) = \mathfrak{L}\{w(t,x,y)\}$. Upon (22), we write (21) in the form:

$$\begin{aligned} &s^{\beta}\frac{\partial \mathscr{W}(s,x,y)}{\partial x} - s^{\beta-1}\frac{\partial w_0(x,y)}{\partial x} + \mu_1 \frac{\partial^4 \mathscr{W}(s,x,y)}{\partial x^4} + \mu_2 \frac{\partial^4 \mathscr{W}(s,x,y)}{\partial x^3 \partial y} \\ &+ 6\mu_1 \mathfrak{L}\left\{\frac{\partial^2 \mathfrak{L}^{-1}\{\mathscr{W}(s,x,y)\}}{\partial x^2}\frac{\partial \mathfrak{L}^{-1}\{\mathscr{W}(s,x,y)\}}{\partial x}\right\} \\ &+ 4\mu_2 \mathfrak{L}\left\{\frac{\partial^2 \mathfrak{L}^{-1}\{\mathscr{W}(s,x,y)\}}{\partial x \partial y}\frac{\partial \mathfrak{L}^{-1}\{\mathscr{W}(s,x,y)\}}{\partial x}\right\} \\ &+ 4\mu_2 \mathfrak{L}\left\{\frac{\partial^2 \mathfrak{L}^{-1}\{\mathscr{W}(s,x,y)\}}{\partial x^2}\frac{\partial \mathfrak{L}^{-1}\{\mathscr{W}(s,x,y)\}}{\partial y}\right\} = 0. \end{aligned} \tag{23}$$

Consequently, (23) rewrite in the following form:

$$\frac{\partial \mathscr{W}(s,x,y)}{\partial x} - \frac{1}{s}\frac{\partial w_0(x,y)}{\partial x} + \frac{1}{s^{\beta}}\left(\mu_1 \frac{\partial^4 \mathscr{W}(s,x,y)}{\partial x^4} + \mu_2 \frac{\partial^4 \mathscr{W}(s,x,y)}{\partial x^3 \partial y}\right.$$

$$+6\mu_1\mathfrak{L}\left\{\frac{\partial^2\mathfrak{L}^{-1}\{\mathscr{W}(s,x,y)\}}{\partial x^2}\frac{\partial\mathfrak{L}^{-1}\{\mathscr{W}(s,x,y)\}}{\partial x}\right\}$$

$$+4\mu_2\mathfrak{L}\left\{\frac{\partial^2\mathfrak{L}^{-1}\{\mathscr{W}(s,x,y)\}}{\partial x\partial y}\frac{\partial\mathfrak{L}^{-1}\{\mathscr{W}(s,x,y)\}}{\partial x}\right\}$$

$$+4\mu_2\mathfrak{L}\left\{\frac{\partial^2\mathfrak{L}^{-1}\{\mathscr{W}(s,x,y)\}}{\partial x^2}\frac{\partial\mathfrak{L}^{-1}\{\mathscr{W}(s,x,y)\}}{\partial y}\right\}\Bigg)=0. \tag{24}$$

We assume the solution for the equation (24) in the form:

$$\mathscr{W}(s,x,y)=\sum_{p=0}^{\infty}\frac{A_p(x,y)}{s^{p\beta+1}},\ s>0. \tag{25}$$

Utilizing part (1) in Lemma 2 to obtain the initial coefficient in the series (25) as: $A_0(x,y)=w_0(x,y)$. Thus, the solution (25) can be written as:

$$\mathscr{W}(s,x,y)=\frac{w_0(x,y)}{s}+\sum_{p=1}^{\infty}\frac{A_p(x,y)}{s^{p\beta+1}},\ s>0. \tag{26}$$

Define the Nth-truncated series of $\mathscr{W}(s,x,y)$ in the form:

$$\mathscr{W}^N(s,x,y)=\frac{w_0(x,y)}{s}+\sum_{p=1}^{N}\frac{A_p(x,y)}{s^{p\beta+1}},\ s>0. \tag{27}$$

Define the Laplace residual function for the equation (24) as:

$\mathfrak{L}\mathfrak{R}es(s)$

$$=\sum_{p=1}^{\infty}\frac{1}{s^{p\beta+1}}\frac{\partial A_p(x,y)}{\partial x}+\frac{1}{s^{\beta}}\Bigg(\frac{\mu_1}{s}\frac{\partial^4 w_0(x,y)}{\partial x^4}$$

$$+\mu_1\sum_{p=1}^{\infty}\frac{1}{s^{p\beta+1}}\frac{\partial^4 A_p(x,y)}{\partial x^4}+\frac{\mu_2}{s}\frac{\partial^4 w_0(x,y)}{\partial x^3\partial y}+\mu_2\sum_{p=1}^{\infty}\frac{1}{s^{p\beta+1}}\frac{\partial^4 A_p(x,y)}{\partial x^3\partial y}$$

$$+6\mu_1\mathfrak{L}\left\{\left(\frac{\partial^2 w_0(x,y)}{\partial x^2}+\mathfrak{L}^{-1}\left\{\sum_{p=1}^{\infty}\frac{1}{s^{p\beta+1}}\frac{\partial^2 A_p(x,y)}{\partial x^2}\right\}\right)\times\left(\frac{\partial w_0(x,y)}{\partial x}+\mathfrak{L}^{-1}\left\{\sum_{p=1}^{\infty}\frac{1}{s^{p\beta+1}}\frac{\partial A_p(x,y)}{\partial x}\right\}\right)\right\}$$

$$+4\mu_2\mathfrak{L}\left\{\left(\frac{\partial^2 w_0(x,y)}{\partial x\partial y}+\mathfrak{L}^{-1}\left\{\sum_{p=1}^{\infty}\frac{1}{s^{p\beta+1}}\frac{\partial^2 A_p(x,y)}{\partial x\partial y}\right\}\right)\times\left(\frac{\partial w_0(x,y)}{\partial x}+\mathfrak{L}^{-1}\left\{\sum_{p=1}^{\infty}\frac{1}{s^{p\beta+1}}\frac{\partial A_p(x,y)}{\partial x}\right\}\right)\right\}$$

$$+4\mu_2\mathfrak{L}\left\{\left(\frac{\partial^2 w_0(x,y)}{\partial x^2}+\mathfrak{L}^{-1}\left\{\sum_{p=1}^{\infty}\frac{1}{s^{p\beta+1}}\frac{\partial^2 A_p(x,y)}{\partial x^2}\right\}\right)\times\left(\frac{\partial w_0(x,y)}{\partial y}+\mathfrak{L}^{-1}\left\{\sum_{p=1}^{\infty}\frac{1}{s^{p\beta+1}}\frac{\partial A_p(x,y)}{\partial y}\right\}\right)\right\}\Bigg). \tag{28}$$

Consequently, the Nth- Laplace residual function for the equation (24) given as:

$$\begin{aligned}
&\mathfrak{L}\mathfrak{R}es^N(s)\\
&=\sum_{p=1}^{N}\frac{1}{s^{p\beta+1}}\frac{\partial A_p(x,y)}{\partial x}+\frac{1}{s^\beta}\left(\frac{\mu_1}{s}\frac{\partial^4 w_0(x,y)}{\partial x^4}\right.\\
&+\mu_1\sum_{p=1}^{N}\frac{1}{s^{p\beta+1}}\frac{\partial^4 A_p(x,y)}{\partial x^4}+\frac{\mu_2}{s}\frac{\partial^4 w_0(x,y)}{\partial x^3\partial y}+\mu_2\sum_{p=1}^{N}\frac{1}{s^{p\beta+1}}\frac{\partial^4 A_p(x,y)}{\partial x^3\partial y}\\
&+6\mu_1\mathfrak{L}\left\{\left(\frac{\partial^2 w_0(x,y)}{\partial x^2}+\mathfrak{L}^{-1}\left\{\sum_{p=1}^{N}\frac{1}{s^{p\beta+1}}\frac{\partial^2 A_p(x,y)}{\partial x^2}\right\}\right)\times\left(\frac{\partial w_0(x,y)}{\partial x}+\mathfrak{L}^{-1}\left\{\sum_{p=1}^{N}\frac{1}{s^{p\beta+1}}\frac{\partial A_p(x,y)}{\partial x}\right\}\right)\right\}\\
&+4\mu_2\mathfrak{L}\left\{\left(\frac{\partial^2 w_0(x,y)}{\partial x\partial y}+\mathfrak{L}^{-1}\left\{\sum_{p=1}^{N}\frac{1}{s^{p\beta+1}}\frac{\partial^2 A_p(x,y)}{\partial x\partial y}\right\}\right)\times\left(\frac{\partial w_0(x,y)}{\partial x}+\mathfrak{L}^{-1}\left\{\sum_{p=1}^{N}\frac{1}{s^{p\beta+1}}\frac{\partial A_p(x,y)}{\partial x}\right\}\right)\right\}\\
&\left.+4\mu_2\mathfrak{L}\left\{\left(\frac{\partial^2 w_0(x,y)}{\partial x^2}+\mathfrak{L}^{-1}\left\{\sum_{p=1}^{N}\frac{1}{s^{p\beta+1}}\frac{\partial^2 A_p(x,y)}{\partial x^2}\right\}\right)\times\left(\frac{\partial w_0(x,y)}{\partial y}+\mathfrak{L}^{-1}\left\{\sum_{p=1}^{N}\frac{1}{s^{p\beta+1}}\frac{\partial A_p(x,y)}{\partial y}\right\}\right)\right\}\right).
\end{aligned}\tag{29}$$

According to step VI, we find $A_1(x,y)$ by multiplying $s^{\beta+1}$ by the expression $\mathfrak{L}\mathfrak{R}es^1(s)$ and evaluate the limitations as $s\to\infty$ to get:

$$\begin{aligned}
A_1^{(1,0)}(x,y)=&-4\mu_2 w_0^{(1,0)}(x,y)w_0^{(1,1)}(x,y)-4\mu_2 w_0^{(0,1)}(x,y)w_0^{(2,0)}(x,y)\\
&-6\mu_1 w_0^{(1,0)}(x,y)w_0^{(2,0)}(x,y)-\mu_2 w_0^{(3,1)}(x,y)-\mu_1 w_0^{(4,0)}(x,y),
\end{aligned}\tag{30}$$

where we are using the notation $g^{(i,j)}(x,y)=\frac{\partial^{i+j}g(x,y)}{\partial x^i\partial y^j}$. Integrate (30) with respect to x to obtain:

$$A_1(x,y)=-4\mu_2 w_0^{(0,1)}(x,y)w_0^{(1,0)}(x,y)-3\mu_1 w_0^{(1,0)}(x,y)^2-\mu_2 w_0^{(2,1)}(x,y)-\mu_1 w_0^{(3,0)}(x,y). \tag{31}$$

The rest of the coefficients obtained were as follows:

$$A_2(x,y)=-4\mu_2 {A_1}^{(0,1)}(x,y){w_0}^{(1,0)}(x,y)$$

$$-2\left(2\mu_2 w_0^{(0,1)}(x,y)+3\mu_1 w_0^{(1,0)}(x,y)\right)A_1{}^{(1,0)}(x,y)-\mu_2 A_1{}^{(2,1)}(x,y)$$

$$-\mu_1 A_1{}^{(3,0)}(x,y). \tag{32}$$

$$\begin{aligned}A_3(x,y)=&\mu_2\left(-4A_2{}^{(0,1)}(x,y)w_0^{(1,0)}(x,y)-\frac{4\Gamma(1+2\beta)A_1{}^{(0,1)}(x,y)A_1{}^{(1,0)}(x,y)}{\Gamma(1+\beta)^2}\right.\\&\left.-4w_0^{(0,1)}(x,y)A_2{}^{(1,0)}(x,y)-A_2{}^{(2,1)}(x,y)\right)\\&+\mu_1\left(-\frac{3\Gamma(1+2\beta)A_1{}^{(1,0)}(x,y)^2}{\Gamma(1+\beta)^2}-6w_0^{(1,0)}(x,y)A_2{}^{(1,0)}(x,y)-A_2{}^{(3,0)}(x,y)\right).\end{aligned} \tag{33}$$

$$\begin{aligned}A_4(x,y)=&-4\mu_2 A_3{}^{(0,1)}(x,y)w_0^{(1,0)}(x,y)-\frac{4\Gamma(1+3\beta)\mu_2 A_2{}^{(0,1)}(x,y)A_1{}^{(1,0)}(x,y)}{\Gamma(1+\beta)\Gamma(1+2\beta)}\\&-\frac{2\Gamma(1+3\beta)\left(2\mu_2 A_1{}^{(0,1)}(x,y)+3\mu_1 A_1{}^{(1,0)}(x,y)\right)A_2{}^{(1,0)}(x,y)}{\Gamma(1+\beta)\Gamma(1+2\beta)}\\&-2\left(2\mu_2 w_0^{(0,1)}(x,y)+3\mu_1 w_0^{(1,0)}(x,y)\right)A_3{}^{(1,0)}(x,y)-\mu_2 A_3{}^{(2,1)}(x,y)-\mu_1 A_3{}^{(3,0)}(x,y).\end{aligned} \tag{34}$$

$$\begin{aligned}A_5(x,y)=&-4\mu_2 A_4{}^{(0,1)}(x,y)w_0^{(1,0)}(x,y)-\frac{4\Gamma(1+4\beta)\mu_2 A_3{}^{(0,1)}(x,y)A_1{}^{(1,0)}(x,y)}{\Gamma(1+\beta)\Gamma(1+3\beta)}\\&-\frac{4\Gamma(1+4\beta)\mu_2 A_2{}^{(0,1)}(x,y)A_2{}^{(1,0)}(x,y)}{\Gamma(1+2\beta)^2}-\frac{3\Gamma(1+4\beta)\mu_1 A_2{}^{(1,0)}(x,y)^2}{\Gamma(1+2\beta)^2}\\&-\frac{2\Gamma(1+4\beta)\left(2\mu_2 A_1{}^{(0,1)}(x,y)+3\mu_1 A_1{}^{(1,0)}(x,y)\right)A_3{}^{(1,0)}(x,y)}{\Gamma(1+\beta)\Gamma(1+3\beta)}\\&-2\left(2\mu_2 w_0^{(0,1)}(x,y)+3\mu_1 w_0^{(1,0)}(x,y)\right)A_4{}^{(1,0)}(x,y)-\mu_2 A_4{}^{(2,1)}(x,y)-\mu_1 A_4{}^{(3,0)}(x,y).\end{aligned} \tag{35}$$

$$A_6(x,y)=-4\mu_2 A_5{}^{(0,1)}(x,y)w_0^{(1,0)}(x,y)-\frac{4\Gamma(1+5\beta)\mu_2 A_4{}^{(0,1)}(x,y)A_1{}^{(1,0)}(x,y)}{\Gamma(1+\beta)\Gamma(1+4\beta)}$$

$$-\frac{4\Gamma(1+5\beta)\mu_2 {A_3}^{(0,1)}(x,y){A_2}^{(1,0)}(x,y)}{\Gamma(1+2\beta)\Gamma(1+3\beta)}$$

$$-\frac{2\Gamma(1+5\beta)\left(2\mu_2 {A_2}^{(0,1)}(x,y)+3\mu_1 {A_2}^{(1,0)}(x,y)\right){A_3}^{(1,0)}(x,y)}{\Gamma(1+2\beta)\Gamma(1+3\beta)}$$

$$-\frac{2\Gamma(1+5\beta)\left(2\mu_2 {A_1}^{(0,1)}(x,y)+3\mu_1 {A_1}^{(1,0)}(x,y)\right){A_4}^{(1,0)}(x,y)}{\Gamma(1+\beta)\Gamma(1+4\beta)}$$

$$-2\left(2\mu_2 w_0^{(0,1)}(x,y)+3\mu_1 w_0^{(1,0)}(x,y)\right){A_5}^{(1,0)}(x,y)-\mu_2 {A_5}^{(2,1)}(x,y)-\mu_1 {A_5}^{(3,0)}(x,y). \tag{36}$$

The sixth-order approximation was chosen because it achieves a sufficient level of accuracy for most physical applications, as will be demonstrated in the numerical results presented throughout the work. Furthermore, higher orders of permutations require extremely complex calculations, which is one of the main challenges of the proposed method. The sixth-order approximation strikes a balance between computational cost and accuracy, making it practical for application while maintaining the accuracy of the results. The 6^{th}-truncated series of $\mathscr{W}(s,x,y)$ given as:

$$\mathscr{W}^6(s,x,y)=\frac{w_0(x,y)}{s}+\frac{A_1(x,y)}{s^{\beta+1}}+\frac{A_2(x,y)}{s^{2\beta+1}}+\frac{A_3(x,y)}{s^{3\beta+1}}+\frac{A_4(x,y)}{s^{4\beta+1}}+\frac{A_5(x,y)}{s^{5\beta+1}}+\frac{A_6(x,y)}{s^{6\beta+1}}. \tag{37}$$

Apply the inverse LT for the 6^{th}-truncated series $\mathscr{W}^6(s,x,y)$ in (37), with using Theorem 1 to obtain the 6^{th} LRPS solutions $w^6(t,x,y)$ for the (2 + 1)-dimensional time fractional BK equation (1) in the form:

$$w^6(t,x,y)=w_0(x,y)+\frac{A_1(x,y)t^{\beta}}{\Gamma(\beta+1)}+\frac{A_2(x,y)t^{2\beta}}{\Gamma(2\beta+1)}+\frac{A_3(x,y)t^{3\beta}}{\Gamma(3\beta+1)}+\frac{A_4(x,y)t^{4\beta}}{\Gamma(4\beta+1)}+\frac{A_5(x,y)t^{5\beta}}{\Gamma(5\beta+1)}+\frac{A_6(x,y)t^{6\beta}}{\Gamma(6\beta+1)}. \tag{38}$$

4. Numerical results

In this section we present and discuss some numerical results for the obtained 6^{th} LRPS solutions $w^6(t,x,y)$ in (38) for the (2 + 1)-dimensional time fractional BK equation (1).

Example 1 Consider the exact solution for the (2+1)-dimensional time fractional BK equation (1) as [22]:

$$w(t,x,y)=a_0-\frac{3k\sqrt{-\sigma}a_1}{2\left(\mu_1 k^3\sigma-a_1\right)}\tanh\left(\sqrt{-\sigma}\left(kx+\frac{\left(a_1-4\mu_1 k^3\sigma\right)}{4\mu_2 k^2\sigma}y+a_1\frac{t^{\beta}}{\beta}\right)\right), \tag{39}$$

where a_0, a_1 and k are arbitrary constants and $\sigma<0$. Hence, we assume the initial condition as:

$$w_0(x,y)=a_0-\frac{3k\sqrt{-\sigma}a_1}{2\left(\mu_1 k^3\sigma-a_1\right)}\tanh\left(\sqrt{-\sigma}\left(kx+\frac{\left(a_1-4\mu_1 k^3\sigma\right)}{4\mu_2 k^2\sigma}y\right)\right). \tag{40}$$

Let $a_0=1, a_1=3, k=2, \sigma=-4, \mu_1=2.5$ and $\mu_2=1$. Thus, the initial condition (40) written as:

$$w_0(x,y) = 1 + \frac{18}{83}\tanh\left(4x - \frac{323}{32}y\right). \tag{41}$$

The example we are looking at use the numbers $\mu_1 = 2.5$ and $\mu_2 = 1$ from something that was written before. These numbers are like helpers that tell us how things spread out. If we change μ_1 and μ_2 it will change how strong the spreading effects are. If we make μ_1 bigger it helps things spread out more in the x-direction. This makes the waves get wider and move faster. If we make μ_2 bigger it helps the x and y parts talk to each other more. This makes the different parts interact with each other in a way. The relationship between μ_2 and μ_1 tells us if something is spreading out the same in all directions. If $\mu_2/\mu_1 = 1$, then it is spreading out the same everywhere. We tested the relationship between μ_2 and μ_1. Found that it works when $\mu_2/\mu_1 = 0.4$. This tells us that our method works for things that do not spread out the same in all directions. We think it will work for relationships, between μ_2 and μ_1 too as long as they make sense in the real world. With the aid of the obtained 6^{th} LRPS solutions $w^6(t,x,y)$ in (38) at the selected parameters we present the following figures. Figure 1 shows the 3D and 2D plots for the 6^{th} LRPS solutions $w^6(t,x,y)$ in (38) for the (2 + 1)-dimensional time fractional BK equation (1) at $a_0 = 1, a_1 = 3, k = 2, \sigma = -4, \mu_1 = 2.5,\ \mu_2 = 1, y = 0$ at integer-order derivative order $\beta = 1$. The 3D plot in Figure 1a shows how the solution changes over time t and space x. The waveform starts at a low point and slowly rises until it reaches a high point, like a phase transition or a kink-type solution. The 2D plot in Figure 1b at time $t = 0.1$ clearly shows the sharp change between the minimum and maximum values on the x-axis, which confirms that the solution is transitional. This pattern shows a stable nonlinear response and is a good way to show how physical systems work with a steep transition gradient, like material interfaces or phase transitions.

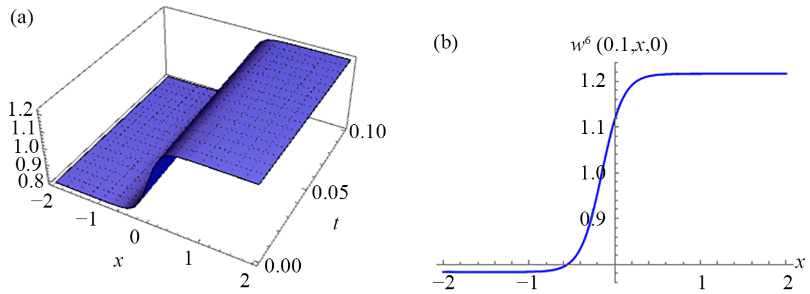

Figure 1. The 6^{th} LRPS solutions $w^6(t, x, y)$ in (38) for the (2 + 1)-dimensional time fractional BK equation (1) at $a_0 = 1,\ a_1 = 3,\ k = 2,\ \sigma = -4,\ \mu_1 = 2.5,\ \mu_2 = 1,\ y = 0$ at integer-order derivative order $\beta = 1$ where: (a) 3D plot; (b) 2D plot at $t = 0.1$

In Figure 2, we compare the obtained 6^{th} LRPS solutions solution $w^6(t,x,y)$ with exact solution (39) at integer-order derivative order $\beta = 1$ at different times $t \in \{0.1, 0.2, 0.3, 0.4\}$. Figure 2a shows that there is agreement between the solutions shown at time $t = 0.1$. We observe that over time, there are fluctuations in the behavior of the inferred solution around the spatial variable $x = 0$ (see Figure 2b–d), and agreement between the solutions at large values of x. This behavior reflects the effects of diffusion, scattering, and nonlinear phenomena in the system. This demonstrates the effectiveness of the proposed method in capturing the initial behavior of the system. To make the comparison process clearer, we calculated and plotted the absolute error between the approximate solution obtained from the proposed method and the exact solution at integer-order derivative order $\beta = 1$. Figure 3 shows a representation of this error at different times. Figures 3a–c show how the absolute error between the LRPS solution and the exact solution of the governing model at $\beta = 1$ changes over time. We can see that the error goes from 10 (for very high accuracy at short time $t = 0.1$ in Figure 3a) to 0.0003 (at longer time $t = 0.5$ in Figure 3c). This shows that the LRPS method is still eligible to obtain accurate solutions even as time goes on. The small rise in error over time is due to the buildup of nonlinear effects.

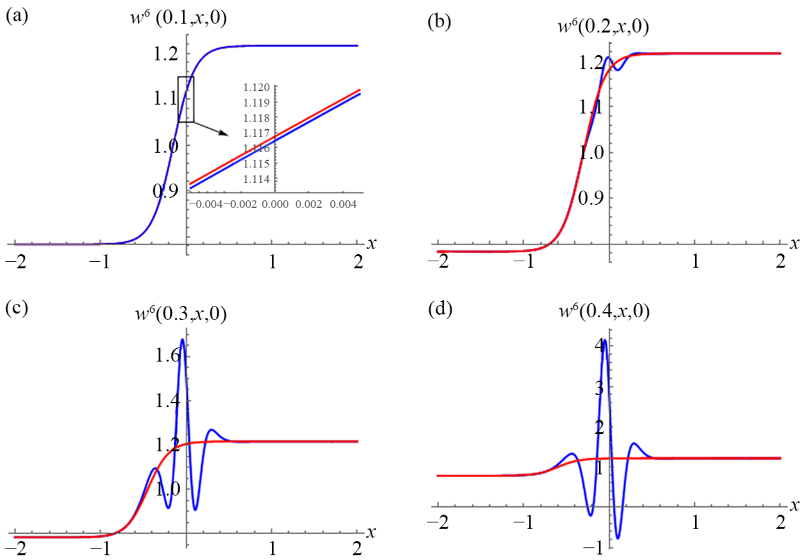

Figure 2. The 6th LRPS solutions $w^6(t, x, y)$ in (38) for the (2 + 1)-dimensional time fractional BK equation (1) (in blue) and exact solution in (39) (in red) at $a_0 = 1,\ a_1 = 3,\ k = 2,\ \sigma = -4,\ \mu_1 = 2.5,\ \mu_2 = 1,\ y = 0$ at integer-order derivative order $\beta = 1$ where: (a) 2D plot at $t = 0.1$; (b) 2D plot at $t = 0.2$; (c) 2D plot at $t = 0.3$; (d) 2D plot at $t = 0.4$

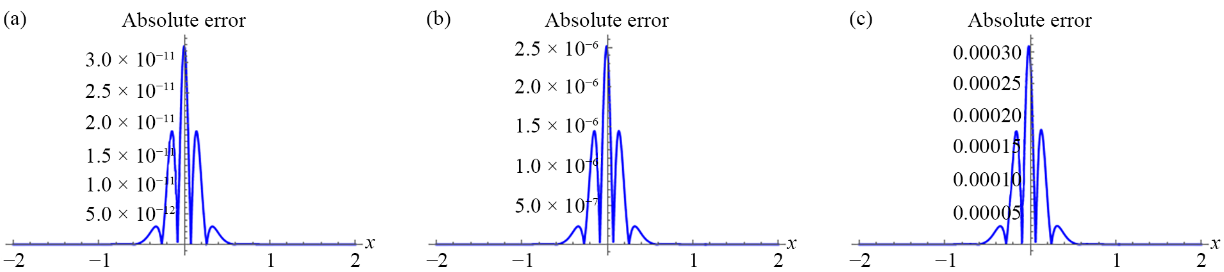

Figure 3. Absolute error between the exact solution (39) and 6th LRPS solutions $w^6(t, x, y)$ in (38) for the (2 + 1)-dimensional time fractional BK equation (1) at $a_0 = 1,\ a_1 = 3,\ k = 2,\ \sigma = -4,\ \mu_1 = 2.5,\ \mu_2 = 1,\ y = 0$ at integer-order derivative order $\beta = 1$ where: (a) $t = 0.01$; (b) $t = 0.05$; (c) $t = 0.1$

Table 1 shows the exact solution, the 4th LRPS solutions $w^4(t,x,y)$ and the 6th LRPS solutions $w^6(t,x,y)$ in (38) for the (2 + 1)-dimensional time fractional BK equation (1) at integer-order derivative order $\beta = 1$ at $a_0 = 1,\ a_1 = 3,\ k = 2,\ \sigma = -4,\ \mu_1 = 2.5,\ \mu_2 = 1,\ y = 0$. Table 2 shows the error analysis for the numerical results obtained in Table 1. The results in Tables 1 and 2 show that the LRPS method works very well for solving the fractional governing model. Table 1 shows that the approximate LRPS solutions, $w^4(t,x,y)$ and $w^6(t,x,y)$, get closer to the exact solution, especially when $t = 0.1$, where the accuracy reaches 9 decimal places. Table 2 goes into detail about the errors. We can see that the absolute and relative errors of the sixth-order approximation $w^6(t,x,y)$ are much smaller than those of the fourth-order approximation $w^4(t,x,y)$. This evidence shows that increasing the approximation order makes it more accurate. The errors do get more as time goes on $t = 0.5$, though, especially in areas where things change quickly (like $x = 0$), where the relative errors are 1.24774 for $w^4(t,x,y)$ and 4.53161 for $w^6(t,x,y)$. This shows how hard it is to model the system's long-term nonlinear behavior. In general, these results show that the LRPS method works well for finding accurate solutions to complicated fractional models. They also show how important it is to use higher orders of approximation to make things more accurate, especially when looking at how the system behaves over time.

Table 1. Numerical results for the exact solution, the 4th and 6th LRPS solutions $w^4(t, x, y)$ and $w^6(t, x, y)$ in (38) for the (2 + 1)-dimensional time fractional BK equation (1) at integer-order derivative order $\beta = 1$

t	x	Exact solution	$w^4(t, x, y)$	$w^6(t, x, y)$
0.1	−2	0.7831326921	0.7831326909	0.7831326921
	−1.5	0.7831413779	0.7831413094	0.7831413756
	−1	0.7836150758	0.7836113854	0.7836149607
	−0.5	0.8079960281	0.8079197263	0.8080019645
	0	1.1164685807	1.1145060240	1.1167545059
	0.5	1.2144878703	1.2144115686	1.2144905880
	1	1.2168236499	1.2168211692	1.2168235635
	1.5	1.2168666672	1.2168666213	1.2168666655
	2	1.2168674551	1.2168674543	1.2168674551
0.5	−2	0.7831522207	0.7831381433	0.7831444691
	−1.5	0.7842049931	0.7834389802	0.7837842571
	−1	0.8348350023	0.7998049562	0.8183593871
	−0.5	1.1651649976	1.5306820884	1.8077945778
	0	1.2157950068	−0.3012048192	6.7253009707
	0.5	1.2168477792	1.0543811359	1.2811984809
	1	1.2168671092	1.2123879463	1.2124886451
	1.5	1.2168674632	1.2167848665	1.2167849005
	2	1.2168674697	1.2168659567	1.2168659567

Table 2. Error analysis for the numerical results obtained in Table 1

t	x	Consecutive Error	Absolute Error		Relative Error	
			4th Absolute Error	6th Absolute Error	4th Relative Error	6th Relative Error
0.1	−2	1.2145×10^{-9}	1.2552×10^{-9}	4.0693×10^{-11}	1.6028×10^{-9}	5.1962×10^{-11}
	−1.5	6.6297×10^{-8}	6.8517×10^{-8}	2.2197×10^{-9}	8.7490×10^{-8}	2.8344×10^{-9}
	−1	3.5753×10^{-6}	3.6904×10^{-6}	1.1511×10^{-7}	4.7095×10^{-6}	1.4690×10^{-7}
	−0.5	8.2238×10^{-5}	7.6301×10^{-5}	5.9364×10^{-6}	9.4433×10^{-5}	7.3471×10^{-6}
	0	2.2484×10^{-3}	1.9625×10^{-3}	2.8592×10^{-4}	1.7578×10^{-3}	2.5609×10^{-4}
	0.5	7.9019×10^{-5}	7.6301×10^{-5}	2.7176×10^{-6}	6.2826×10^{-5}	2.2377×10^{-6}
	1	2.3943×10^{-6}	2.4807×10^{-6}	8.6395×10^{-8}	2.0386×10^{-6}	7.1000×10^{-8}
	1.5	4.4202×10^{-8}	4.5845×10^{-8}	1.6431×10^{-9}	3.7674×10^{-8}	1.3502×10^{-9}
	2	8.0970×10^{-10}	8.3981×10^{-10}	3.0115×10^{-11}	6.9014×10^{-10}	2.4748×10^{-11}
0.5	−2	6.3258×10^{-6}	1.4077×10^{-5}	7.7516×10^{-6}	1.7975×10^{-5}	9.8980×10^{-6}
	−1.5	3.4527×10^{-4}	7.6601×10^{-4}	4.2073×10^{-4}	9.7680×10^{-4}	5.3651×10^{-4}
	−1	1.8554×10^{-2}	3.503×10^{-2}	1.6475×10^{-2}	4.1960×10^{-2}	1.9735×10^{-2}
	−0.5	2.7711×10^{-1}	3.6551×10^{-1}	6.4263×10^{-1}	3.1370×10^{-1}	5.5153×10^{-1}
	0	7.02651	1.517	5.50951	1.24774	4.53161
	0.5	2.2681×10^{-1}	1.6246×10^{-1}	6.4350×10^{-2}	1.3351×10^{-1}	5.2883×10^{-2}
	1	1.0069×10^{-4}	4.4791×10^{-3}	4.3784×10^{-3}	3.6809×10^{-3}	3.5981×10^{-3}
	1.5	3.3950×10^{-8}	8.2596×10^{-5}	8.2562×10^{-5}	6.7876×10^{-5}	6.7848×10^{-5}
	2	1.1389×10^{-11}	1.513×10^{-6}	1.5129×10^{-6}	1.2433×10^{-6}	1.2433×10^{-6}

Figures 4a–c present a comprehensive analysis of LRPS solutions to the governing model at fractional derivative orders $\beta = 0.95, 0.93$, and 0.9. The results show that when the fractional order β is decreased from 0.95 to 0.9, the system

behaves differently, becoming smoother and greatly lowering the highest values, highlighting the long memory effect common in fractional systems. Figures 5a–c show how the LRPS solutions solution $w^6(t,x,y)$ of the governing model has changed over time in 2D plots. The study shows that lowering the fractional β from 0.95 to 0.9 makes the system behave differently. The solutions bounce less and the differences for values of x between -2 and 2 drop a lot. When we compare the red curves at $t = 0.08$ to the blue curves at $t = 0.05$, we can see these effects more clearly. The solution changes more slowly over time because the system has fractional properties. Physically, these changes represent an increase in energy dissipation within plasma systems and a modification of the viscous properties of the fluids. They also demonstrate a slowdown in diffusion and transport processes. These results are particularly intriguing for applications such as modeling astronomical plasma behavior and studying diffusion in porous media, as they demonstrate a remarkable agreement with experimental observations and theoretical models of fractional systems.

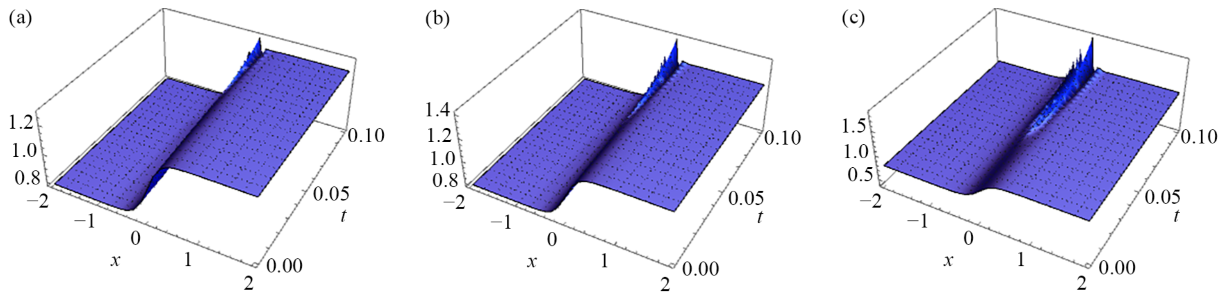

Figure 4. The 6th LRPS solutions $w^6(t,x,y)$ in (38) for the (2 + 1)-dimensional time fractional BK equation (1) at $a_0 = 1,\ a_1 = 3,\ k = 2,\ \sigma = -4,\ \mu_1 = 2.5,\ \mu_2 = 1,\ y = 0$ at different fractional order derivative order β where (a) $\beta = 0.95$; (b) $\beta = 0.93$; (c) $\beta = 0.9$

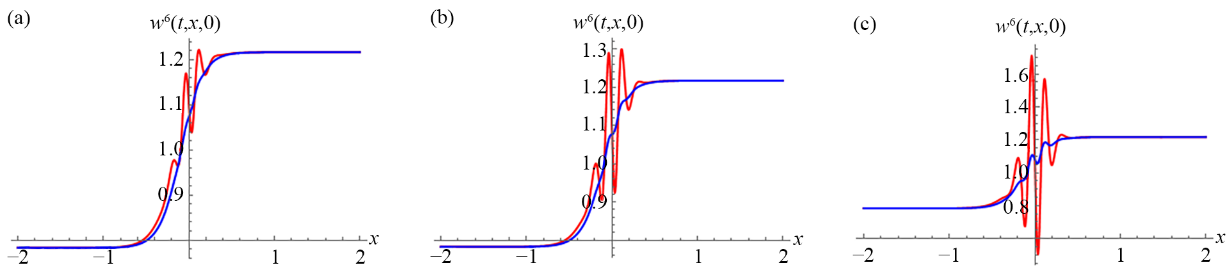

Figure 5. The 6th LRPS solutions $w^6(t,x,y)$ in (38) for the (2 + 1)-dimensional time fractional BK equation (1) at $a_0 = 1,\ a_1 = 3,\ k = 2,\ \sigma = -4,\ \mu_1 = 2.5,\ \mu_2 = 1,\ y = 0$ at different fractional order derivative order β at $t = 0.08$ in red and $t = 0.05$ in blue where (a) $\beta = 0.95$; (b) $\beta = 0.93$; (c) $\beta = 0.9$

Example 2 Consider the exact solution for the (2 + 1)-dimensional time fractional BK equation (1) as [22]:

$$w(t,x,y) = a_0 + \frac{3k\sqrt{\sigma}a_1}{2(\mu_1 k^3\sigma - a_1)}\coth\left(\sqrt{\sigma}\left(kx + \frac{(a_1 - 4\mu_1 k^3\sigma)}{4\mu_2 k^2\sigma}y + a_1\frac{t^\beta}{\beta}\right)\right), \tag{42}$$

where a_0, a_1 and k are arbitrary constants and $\sigma > 0$. Hence, we assume the initial condition as:

$$w_0(x,y) = a_0 + \frac{3k\sqrt{\sigma}a_1}{2(\mu_1 k^3\sigma - a_1)}\coth\left(\sqrt{\sigma}\left(kx + \frac{(a_1 - 4\mu_1 k^3\sigma)}{4\mu_2 k^2\sigma}y\right)\right). \tag{43}$$

Let $a_0 = 1, a_1 = 3, k = 2, \sigma = -4, \mu_1 = 2.5$ and $\mu_2 = 1$. Thus, the initial condition (43) is written as:

$$w_0(x,y) = 1 - \frac{18}{83}\coth\left(4x - \frac{323y}{32}\right). \tag{44}$$

With the aid of the obtained 6$^{\text{th}}$ LRPS solutions $w^6(t,x,y)$ in (38) at the selected parameters we present the following figures.

Figures 6a,b show that the exact solution in (42) and the LRPS solution $w^6(t,x,y)$ at $a_0 = 1,\ a_1 = 3,\ k = 2,\ \sigma = -4,\ \mu_1 = 2.5,\ y = 0$ for the governing model agree well at short times $t = 0.001$. The approximate solution $w^6(t,x,y)$ keeps all the important features of the system, such as the amplitude values (from -5 to 10), the fact that it is spatially symmetric around $x = 0$. This shows that the LRPS method works well with changed initial conditions and can give exact answers even in very short amounts of time. Figure 7 shows a comparison between the exact solution in (42) and the LRPS solution $w^6(t,x,y)$ for the governing model with a fractional derivative order of $\beta = 0.9$ and a short time $t = 0.001$. The comparison shows that the basic structure of the solutions is generally the same, with small differences that show how the fractional nature of the system affects them. Both solutions keep the same general pattern for peaks (around 10) and troughs (around -5), but there are relative differences amplitude, especially at the critical point at $x = 0$. The reason for these differences is that the long memory property of fractional systems changes how energy spreads out across the system.

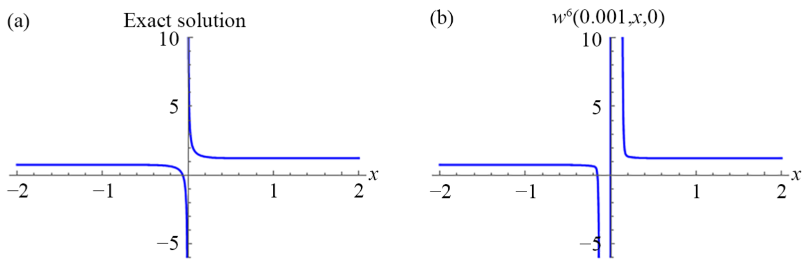

Figure 6. The exact solution in (42) and 6$^{\text{th}}$ LRPS solutions $w^6(t, x, y)$ in (38) for the (2 + 1)-dimensional time fractional BK equation (1) at $a_0 = 1,\ a_1 = 3,\ k = 2,\ \sigma = 4,\ \mu_1 = 2.5,\ \mu_2 = 1,\ y = 0,\ t = 0.001$ at integer-order derivative order $\beta = 1$ where: (a) exact solution; (b) 6$^{\text{th}}$ LRPS solutions $w^6(t, x, y)$

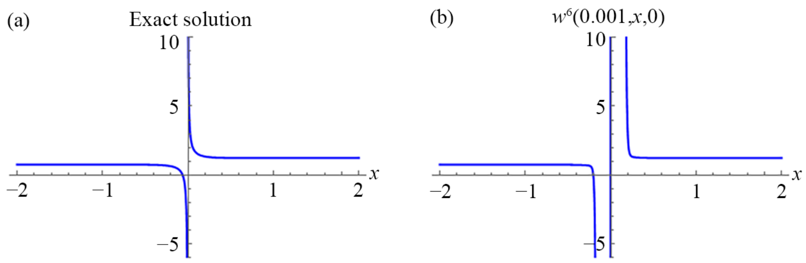

Figure 7. The exact solution in (42) and 6$^{\text{th}}$ LRPS solutions $w^6(t, x, y)$ in (38) for the (2 + 1)-dimensional time fractional BK equation (1) at $a_0 = 1,\ a_1 = 3,\ k = 2,\ \sigma = 4,\ \mu_1 = 2.5,\ \mu_2 = 1,\ y = 0,\ t = 0.001$ at fractional-order derivative order $\beta = 0.9$ where: (a) exact solution; (b) 6$^{\text{th}}$ LRPS solutions $w^6(t, x, y)$

Figures 8a–c show how the approximate solution $w^6(t,x,y)$ of the governing model changes over time $t = 0.01,\ 0.1$, and 0.5 and for values $\beta = 0.9,\ 0.75$, and 0.5. The values range from -5 to 10, with the main peak around $x \approx \pm 2$ and the troughs around $x \approx \pm 4$. As time goes on, the solution spreads out horizontally, and its properties change depending on the order of the fractionalization. At $\beta = 0.9$, the peak stays sharp, and there is a little damping at higher times. At $\beta = 0.75$, the amplitude slowly goes down, and the solution gets smoother. At $\beta = 0.5$, the waveform starts to look like a straight line in the middle and then stretches out over time. This behavior is caused by the long memory that comes with a lower β.

This makes energy move more slowly and increases damping. The results also show that the numerical solutions are still stable even after these changes. Figure 9 makes it clear that the 4^{th} LRPS solution $w^4(t,x,y)$ and the 6^{th} LRPS solution $w^6(t,x,y)$ work differently. The solutions look very similar at first, but as time goes on, they start to look very different. The solution $w^6(t,x,y)$ keeps its coherence and basic structure better, but the solution $w^4(t,x,y)$ starts to lose some fine details and slowly changes shape. The solution $w^6(t,x,y)$ is better at keeping the properties of the fractional system, like how the peaks, troughs, and transition regions act. This means that it can better show how the system changes over time. On the other hand, the solution $w^4(t,x,y)$ does a good job of showing how complex the system is over time, but it doesn't do a good job of doing so over short periods of time. These observations show that the method works better at accurately simulating fractal properties when the approximation is of a higher order. This is especially true over long periods of time, when long-memory effects become more noticeable and important.

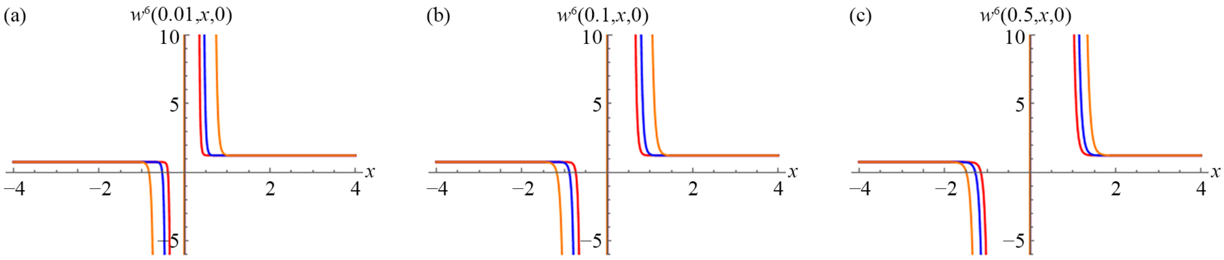

Figure 8. The 6^{th} LRPS solutions $w^6(t, x, y)$ in (38) for the (2 + 1)-dimensional time fractional BK equation (1) at $a_0 = 1,\ a_1 = 3,\ k = 2,\ \sigma = 4,\ \mu_1 = 2.5,\ \mu_2 = 1,\ y = 0$ at different fractional order derivative order $\beta = 0.9$ (in red), $\beta = 0.75$ (in blue) and $\beta = 0.5$ (in orange) where (a) $t = 0.01$; (b) $t = 0.1$; (c) $t = 0.5$

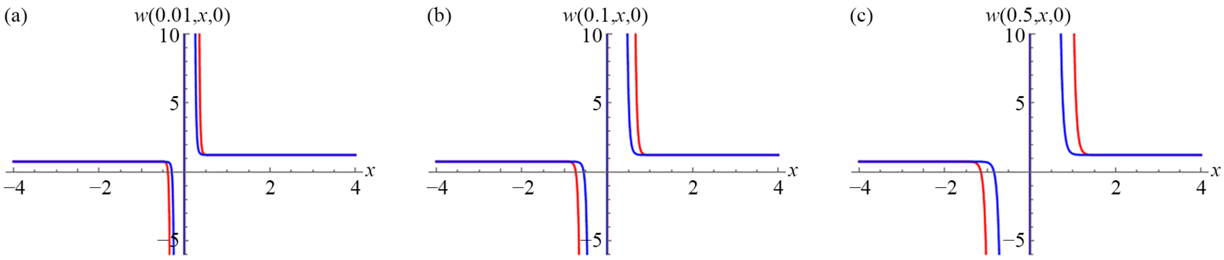

Figure 9. The 6^{th} LRPS solutions $w^6(t, x, y)$ (in red) and 4^{th} LRPS solutions $w^4(t, x, y)$ (in blue) for the (2 + 1)-dimensional time fractional BK equation (1) at $a_0 = 1,\ a_1 = 3,\ k = 2,\ \sigma = 4,\ \mu_1 = 2.5,\ \mu_2 = 1,\ y = 0$ at fractional order derivative order $\beta = 0.9$ where (a) $t = 0.01$; (b) $t = 0.1$; (c) $t = 0.5$

Tables 3–5 show a full analysis of how accurate the approximate solutions to the fractional model (1) are. The analysis of the consecutive, absolute, and relative errors shows that the approximate solution $w^6(t,x,y)$ is much more accurate and stable than the solution $w^4(t,x,y)$, especially at large times $t \to 1.0$ and in areas with complicated dynamical behavior (around $x = \pm 3$). The results show that the errors get bigger over time because of the long memory effects that are common in fractional systems. The relative errors near $x = \pm 3$ are about 10^{-5}, but they are still very small (up to 10^{-12}) in the far regions ($x = \pm 5$). This study shows that using higher orders of approximation, like $w^6(t,x,y)$, makes the results much more accurate, especially in important parts of the model. It also shows that the results stay very stable even when they are used over long periods of time. The results also show that the model is very sensitive to near points with steep gradients.

Table 3. Consecutive error for the 6th LRPS solutions $w^6(t, x, y)$ and 4th LRPS solutions $w^4(t, x, y)$ for the (2 + 1)-dimensional time fractional BK equation (1) at fractional derivative order $\beta = 0.9$

t	x			
	−5	5	−3	3
0.1	0	0	1.7822×10^{-12}	3.5245×10^{-12}
0.2	0	0	2.3252×10^{-11}	9.6824×10^{-11}
0.3	0	2.2204×10^{-16}	4.3722×10^{-11}	7.0078×10^{-10}
0.4	1.1102×10^{-16}	2.2204×10^{-16}	1.9475×10^{-10}	2.9117×10^{-9}
0.5	2.2204×10^{-16}	1.1102×10^{-15}	1.4745×10^{-9}	8.8909×10^{-9}
0.6	5.5511×10^{-16}	2.6645×10^{-15}	5.4488×10^{-9}	2.2295×10^{-8}
0.7	1.6653×10^{-15}	5.7731×10^{-15}	1.5034×10^{-8}	4.8745×10^{-8}
0.8	3.9968×10^{-15}	1.0880×10^{-14}	3.4845×10^{-8}	9.6325×10^{-8}
0.9	8.2156×10^{-15}	1.9762×10^{-14}	7.1663×10^{-8}	1.7611×10^{-7}
1	1.5099×10^{-14}	3.3750×10^{-14}	1.3493×10^{-7}	3.0274×10^{-7}

Table 4. Absolute error for the 6th LRPS solutions $w^6(t, x, y)$ and 4th LRPS solutions $w^4(t, x, y)$ for the (2 + 1)-dimensional time fractional BK equation (1) at fractional derivative order $\beta = 0.9$

t	x			
	−5	5	−3	3
0.1	0	0	9.0116×10^{-11}	9.1092×10^{-11}
0.2	1.1102×10^{-16}	0	3.8983×10^{-10}	4.2722×10^{-10}
0.3	2.2204×10^{-16}	2.2204×10^{-16}	1.4593×10^{-9}	1.6082×10^{-9}
0.4	5.5511×10^{-16}	4.4408×10^{-16}	5.2975×10^{-9}	4.9435×10^{-9}
0.5	2.2204×10^{-15}	1.5543×10^{-15}	1.9439×10^{-8}	1.2842×10^{-8}
0.6	7.9936×10^{-15}	3.3306×10^{-15}	7.1579×10^{-8}	2.9245×10^{-8}
0.7	2.9309×10^{-14}	6.8833×10^{-15}	2.5964×10^{-7}	6.0085×10^{-8}
0.8	1.0347×10^{-13}	1.2878×10^{-14}	9.1933×10^{-7}	1.1379×10^{-7}
0.9	3.5738×10^{-13}	2.2648×10^{-14}	3.1760×10^{-6}	2.0180×10^{-7}
1	1.2089×10^{-12}	3.7969×10^{-14}	1.0741×10^{-5}	3.3916×10^{-7}

Table 5. Relative error for the 6th LRPS solutions $w^6(t, x, y)$ and 4th LRPS solutions $w^4(t, x, y)$ for the (2 + 1)-dimensional time fractional BK equation (1) at fractional derivative order $\beta = 0.9$

t	x			
	−5	5	−3	3
0.1	0	0	1.1760×10^{-10}	7.3833×10^{-11}
0.2	1.4489×10^{-16}	0	5.0877×10^{-10}	3.4627×10^{-10}
0.3	2.8978×10^{-16}	1.7997×10^{-16}	1.9046×10^{-9}	1.3035×10^{-9}
0.4	7.2446×10^{-16}	3.5994×10^{-16}	6.9137×10^{-9}	4.0068×10^{-9}
0.5	2.8978×10^{-15}	1.2598×10^{-15}	2.5370×10^{-8}	1.0409×10^{-8}
0.6	1.0432×10^{-14}	2.6995×10^{-15}	9.3417×10^{-8}	2.3704×10^{-8}
0.7	3.8251×10^{-14}	5.5791×10^{-15}	3.3886×10^{-7}	4.8701×10^{-8}
0.8	1.3504×10^{-13}	1.0438×10^{-14}	1.1998×10^{-6}	9.2229×10^{-8}
0.9	4.6641×10^{-13}	1.8357×10^{-14}	4.145×10^{-6}	1.6356×10^{-7}
1	1.5777×10^{-12}	3.0775×10^{-14}	1.4019×10^{-5}	2.749×10^{-7}

5. Physical interpretations

In this section, we provide some interpretations of the physical behavior reflected by the solutions obtained using the proposed approach to the governing model.

Example 3 Consider the obtained 6^{th} LRPS solution for the (2 + 1)-dimensional time fractional BK equation (1) using the initial condition and the parameters as in Example 1 in Section 4. We obtain the energy function $\mathscr{E}(t,x,y)$ as:

$$\mathscr{E}(t,x,y) = \frac{1}{2}\left(\left(w_x^2(t,x,y)\right)^2 + (w_y^2(t,x,y)^2\right). \tag{45}$$

The energy function at different times is plotted and shown in Figure 10. Figure 10 presents the energy function $\mathscr{E}(t,x,y)$ in (44) obtained from the 6^{th} LRPS solution for the (2 + 1)-dimensional time fractional BK equation (1) at $t \in \{1.2, 1.4, 1.6, 1.8\}$ and we compare the spatial energy evolution between two cases: classical case $\beta = 1$; Figure 10a and fractional case $\beta = 0.9$; Figure 10b.

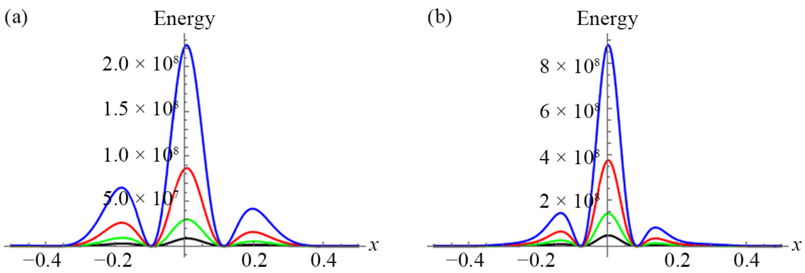

Figure 10. The energy function $\mathscr{E}(t, x, y)$ in (44) for the (2 + 1)-dimensional time fractional BK equation (1) at $a_0 = 1,\ a_1 = 3,\ = 2,\ \sigma = -4,\ \mu_1 = 2.5,\ \mu_2 = 1,\ y = 0$ at $t = 1.2$ (in black), $t = 1.4$ (in green), $t = 1.6$ (in red) and $t = 1.8$ (in blue) where: (a) integer order derivative $\beta = 1$; (b) fractional-order derivative order $\beta = 0.9$

We can see from Figure 10 that the energy wave increases with time. We clearly see that the peak of the curve rises at each subsequent time instant, indicating that energy is accumulating at the center of the wave packet over time. This type of behavior is common in nonlinear systems with self-reinforcing wave interactions. For example, the nonlinear terms in the governing equation ($w_{xx}w_x$, $w_{xy}w_x$) act to transfer energy and concentrate it at the center of space over time. The evolution of the energy function is compared for two cases, with Figure 10 a using the classical order $\beta = 1$ and Figure 10 b using a fractional order $\beta = 0.9$. It is noted that decreasing the value of β slows down the energy accumulation, because the energy peaks are lower at each instant compared to the classical situation. This demonstrates the importance of the fractional time derivative in determining the speed of energy evolution and how the effects propagate over time. It also shows how the fractional derivative reflects memory effects in fractional models.

Example 4 Consider the obtained 6^{th} LRPS solution for the (2 + 1)-dimensional time fractional BK equation (1) using the initial condition and the parameters as in Example 2 in Section 4. We obtain the energy function $\mathscr{E}(t,x,y)$ as (44). Figure 11 shows the evolution of energy function at different times at classical and fractional derivative β.

We used different initial conditions, $w_0(t, x)$ in (44), in this case compared to the previous ones. We then examined the equivalent energy $\mathscr{E}(t, x, y)$ over longer time intervals, ranging from $t = 1$ (black curve) to $t = 15$ (blue curve). The results show that the energy slowly rises over time and stays focused around two symmetrical points on either side of the $x = 0$ axis. This means that the energy has a double-peak localization behavior. These results show that the initial conditions caused a double-peak localization pattern to form. This means that energy builds up in two specific areas without spreading out too much in the horizontal direction. As time goes on, the energy in both peaks rises, but the width of the peaks stays about the same. This suggests that the system is in a localized metastable state where the energy changes without spreading out horizontally. This behavior is a unique type of solution to fractional nonlinear equations, and it is similar to the states called solitary trapped modes or localized energy states in the physics literature. The fact that energy doesn't spread out much over time also supports the idea that fractional order and time work together to keep the energy interaction in the model in a certain balance.

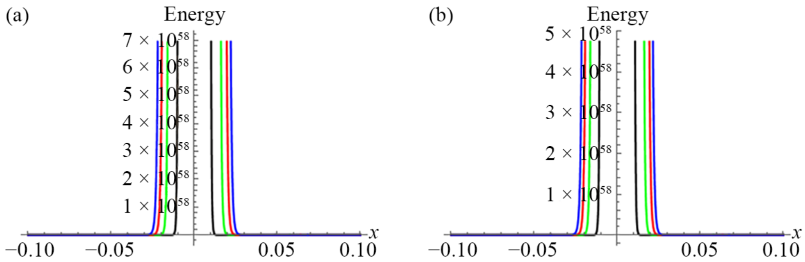

Figure 11. The energy function $\mathscr{E}(t, x, y)$ in (44) for the (2 + 1)-dimensional time fractional BK equation (1) at $a_0 = 1,\ a_1 = 3,\ k = 2,\ \sigma = 4,\ \mu_1 = 2.5,\ \mu_2 = 1,\ y = 0$ at $t = 1$ (in black), $t = 5$ (in green), $t = 10$ (in red) and $t = 15$ (in blue) where: (a) integer order derivative $\beta = 1$; (b) fractional-order derivative order $\beta = 0.9$

When you look at the two figures, you can see how the fractional derivative affects the way the energy changes over time. The first graph has $\beta = 1$ and the second graph has $\beta = 0.9$. In the classical case with $\beta = 1$, the results show a faster rate of energy growth, with energy peaks reaching values that are more than 7×10^{58}. In the fractional case with $\beta = 0.9$, the pattern of spatial energy accumulation stays the same in both location and shape, but the peaks are shorter and the rate of growth over time is slower. The "time memory" property of the fractional derivative is what makes the energy performance of the two cases different. When the system is fractional, its time history constantly affects it, which slows down the distribution of energy and causes non-local damping effects to show up over time. To put it another way, the fractional derivative gives the model the power to control how quickly energy builds up. This is important when simulating physical systems with complicated time properties. So, adding the fractional derivative to the model is a good way to control how energy behaves. It can also be used to simulate materials or media that are viscous or don't respond right away, like non-equilibrium plasmas or composite materials.

6. Conclusions

In this work, we conduct a comprehensive analytical study of the (2 + 1)-dimensional time fractional BK equation (1) using the LRPS method. The proposed approach is applied to generate analytical solutions for the governing equation. The results are presented in figures that illustrate the behavior of the solutions in three- and two-dimensional graphs at different values of the spatial and temporal variables. In addition, tables representing the numerical results of consecutive, absolute, and relative error analyses are presented to achieve a clear comparison between the exact and approximate solutions. From this work, it can be concluded that the proposed method is very effective and highly successful in producing approximate solutions that are in high agreement with the exact solutions. The results presented throughout the paper also demonstrate that as the order of approximation increases, the solutions become more stable compared to lower orders, especially over longer time intervals. Furthermore, we study the effect of the fractional derivative on the behavior of the system, as it adds a gradual damping to the behavior of the solutions, while solutions at integer orders of derivatives maintain their sharp dynamic properties. The work also addresses the physical application of the derived solutions for the governing system. We calculated the energy evolution function for two different cases and demonstrated, through the presented figures, the effect of the fractional derivative on the energy evolution resulting from interactions within the system. As a future direction for this work, it is important to explore and develop numerical methods for dealing with fractional systems that describe complex physical phenomena, such as the governing model presented here. Furthermore, studying the governing model within the context of a different definition of the fractional derivative and comparing the new results with those found in the literature will help in understanding the effects of fractional memory on system dynamics. Since linking numerical results with physical applications of mathematical models provides a complete picture, one future direction involves researching physical applications of the governing model and leveraging the numerical results presented in this work to connect them with these applications.

Acknowledgment

This research has been funded by Scientific Research Deanship at University of Hail-Saudi Arabia through project number (RG-25 062).

Author contributions

Conceptualization (Saleh Alshammari), Methodology (M. Mossa Al-sawalha), Investigation (Mohammad Alshammari), Formal Analysis (Yousef Jawarneh), Writing—Original Draft (Saleh Alshammari and Mohammed Alabedalhadi), Writing—Review & Editing (Mohammed Al-Smadi), Supervision (Mohammed Al-Smadi).

Conflict of interest

The authors declare no competing financial interest.

References

[1] Lü X, Li J. Integrability with symbolic computation on the Bogoyavlensky–Konoplechenko model: bell-polynomial manipulation, bilinear representation, and Wronskian solution. *Nonlinear Dynamics*. 2014; 77(1): 135–143. Available from: https://doi.org/10.1007/s11071-014-1279-3.

[2] Liu JG, Osman MS. Nonlinear dynamics for different nonautonomous wave structures solutions of a 3D variable-coefficient generalized shallow water wave equation. *Chinese Journal of Physics*. 2022; 77: 1618–1624. Available from: https://doi.org/10.1016/j.cjph.2021.10.026.

[3] Hu X, Lin S, Wang L. Integrability, multiple-cosh, lumps and lump-soliton solutions to a (2+1)-dimensional generalized breaking soliton equation. *Communications in Nonlinear Science and Numerical Simulation*. 2020; 91: 105447. Available from: https://doi.org/10.1016/j.cnsns.2020.105447.

[4] Li Q, Chaolu T, Wang YH. Lump-type solutions and lump solutions for the (2+1)-dimensional generalized Bogoyavlensky–Konopelchenko equation. *Computers and Mathematics with Applications*. 2019; 77(8): 2077–2085. Available from: https://doi.org/10.1016/j.camwa.2018.12.011.

[5] Kumar M, Srivastava S, Tanwar DV. Lie symmetries, soliton dynamics, conservation laws and stability analysis of Bogoyavlensky–Konoplechenko system. *Optical and Quantum Electronics*. 2024; 56(7): 1–25. Available from: https://doi.org/10.1007/s11082-024-06990-8.

[6] Vivas-Cortez M, Aftab M, Abbas M, Alosaimi M. Abundant solutions to the generalized reaction duffing model and their applications. *Symmetry*. 2024; 16(7): 847. Available from: https://doi.org/10.3390/sym16070847.

[7] Elboree MK. Soliton solutions for some nonlinear partial differential equations in mathematical physics using He's variational method. *International Journal of Nonlinear Sciences and Numerical Simulation*. 2020; 21(2): 147–158. Available from: https://doi.org/10.1515/ijnsns-2018-0188.

[8] Kumar R, Pandey KS, Yadav SK, Kumar A. Some more variety of analytical solutions to (2+1)-Bogoyavlensky-Konopelchenko equation. *Physica Scripta*. 2024; 99(4): 045240. Available from: https://doi.org/10.1088/1402-4896/ad32fd.

[9] Wang K. Solitary wave dynamics of the local fractional Bogoyavlensky–Konopelchenko model. *Fractals*. 2023; 31(05): 2350054. Available from: https://doi.org/10.1142/S0218348X23500548.

[10] Iqbal N, Alshammari S, Botmart T. Evaluation of regularized long-wave equation via Caputo and Caputo-Fabrizio fractional derivatives. *AIMS Mathematics*. 2022; 7(11): 20401–20419. Available from: https://doi.org/10.3934/math.20221118.

[11] Rashed AS, Mohamed M, Inc M. Plasma particles dispersion based on Bogoyavlensky-Konopelchenko mathematical model. *Computational Methods for Differential Equations*. 2024; 12(3): 561–570. Available from: https://doi.org/10.22034/cmde.2023.54839.2280.

[12] Akram S, Ahmad J, Rehman SU, Ali A. New family of solitary wave solutions to new generalized Bogoyavlensky–Konopelchenko equation in fluid mechanics. *International Journal of Applied and Computational Mathematics*. 2023; 9(5): 63. Available from: https://doi.org/10.1007/s40819-023-01542-2.

[13] Wang K. Solitary wave dynamics of the local fractional Bogoyavlensky–Konopelchenko model. *Fractals*. 2023; 31(05): 2350054. Available from: https://doi.org/10.1142/S0218348X23500548.

[14] Khater MMA, Ghanbari B, Nisar KS, Kumar D. Novel exact solutions of the fractional Bogoyavlensky–Konopelchenko equation involving the Atangana-Baleanu-Riemann derivative. *Alexandria Engineering Journal*. 2020; 59(5): 2957–2967. Available from: https://doi.org/10.1016/j.aej.2020.03.032.

[15] Yokuş A, Duran S, Kaya D. An expansion method for generating travelling wave solutions for the (2+1)-dimensional Bogoyavlensky-Konopelchenko equation with variable coefficients. *Chaos, Solitons and Fractals*. 2024; 178: 114316. Available from: https://doi.org/10.1016/j.chaos.2023.114316.

[16] Ren B, Ma WX, Yu J. Lump solutions for two mixed Calogero-Bogoyavlenskii-Schiff and Bogoyavlensky-Konopelchenko equations. *Communications in Theoretical Physics*. 2019; 71(6): 658. Available from: https://doi.org/10.1088/0253-6102/71/6/658.

[17] Ray SS. On conservation laws by Lie symmetry analysis for (2+1)-dimensional Bogoyavlensky–Konopelchenko equation in wave propagation. *Computers and Mathematics with Applications*. 2017; 74(6): 1158–1165. Available from: https://doi.org/10.1016/j.camwa.2017.06.007.

[18] Mohanty SK, Pradhan B, Sagidullayeva Z, Myrzakulov R, Dev AN. Exact solutions for the Bogoyavlensky-Konopelchenko equation with variable coefficients with an efficient technique. *Alexandria Engineering Journal*. 2023; 72: 287–293. Available from: https://doi.org/10.1016/j.aej.2023.04.001.

[19] Khalique CM, Adeyemo OD, Maefo K. Symmetry solutions and conservation laws of a new generalized 2D Bogoyavlensky-Konopelchenko equation of plasma physics. *AIMS Mathematics*. 2022; 7(6): 9767–9788. Available from: https://doi.org/10.3934/math.2022544.

[20] Manafian J, Mohammadi Ivatloo B, Abapour M. Breather wave, periodic, and cross-kink solutions to the generalized Bogoyavlensky-Konopelchenko equation. *Mathematical Methods in the Applied Sciences*. 2020; 43(4): 1753–1774. Available from: https://doi.org/10.1002/mma.6000.

[21] Ismael HF, Ma WX, Bulut H. Dynamics of soliton and mixed lump-soliton waves to a generalized Bogoyavlensky-Konopelchenko equation. *Physica Scripta*. 2021; 96(3): 035225. Available from: https://doi.org/10.1088/1402-4896/abdc55.

[22] Ali MR, Ma WX, Sadat R. Lie symmetry analysis and invariant solutions for (2+1) dimensional Bogoyavlensky-Konopelchenko equation with variable-coefficient in wave propagation. *Journal of Ocean Engineering and Science*. 2022; 7(3): 248–254. Available from: https://doi.org/10.1016/j.joes.2021.08.006.

[23] Diethelm K. A fractional calculus based model for the simulation of an outbreak of dengue fever. *Nonlinear Dynamics*. 2013; 71: 613–619. Available from: https://doi.org/10.1007/s11071-012-0475-2.

[24] Shafee A, Alkhezi Y, Shah R. Efficient solution of fractional system partial differential equations using Laplace residual power series method. *Fractal and Fractional*. 2023; 7(6): 429. Available from: https://doi.org/10.3390/fractalfract7060429.

[25] Faisal M, Zan-Ul-Abadin Q, Badruddin IA, Ganie AH, Ahmad I, Hussien M. Insight into the bidirectional dynamics of hyperbolic tangent hybrid nanomaterial subject to Nield's conditions using numerical approach. *Numerical Heat Transfer, Part A: Applications*. 2024; 86(21): 7722–7748. Available from: https://doi.org/10.1080/10407782.2024.2353882.

[26] Ganie AH, Wazwaz AM, Seadawy AR, Ullah MS, Afroz HD, Akter R. Application of three analytical approaches to the model of ion sound and Langmuir waves. *Pramana*. 2024; 98(2): 46. Available from: https://doi.org/10.1007/s12043-023-02720-z.

[27] Khan R, Popa IL, Ismail EAA, Awwad FA, Ishtiaq U. Deterministic and fractional-order modeling of measles dynamics with harmonic mean incidence rate and quarantine impact. *Scientific Reports*. 2025; 15(1): 30597. Available from: https://doi.org/10.1038/s41598-025-15253-9.

[28] Iqbal N, Al Harbi MFS, Alshammari S, Zaland S. Analysis of fractional differential equations with the help of different operators. *Advances in Mathematical Physics*. 2022; 2022(1): 1333109. Available from: https://doi.org/10.1155/2022/1333109.

[29] Al-Smadi M, Freihat A, Khalil H, Momani S, Ali Khan R. Numerical multistep approach for solving fractional partial differential equations. *International Journal of Computational Methods*. 2017; 14(03): 1750029. Available from: https://doi.org/10.1142/S0219876217500293.

[30] Al-Sawalha MM, Mukhtar S, Alrowaily AW, Alshammari S, Ismaeel SM, El-Tantawy SA. Analytical solutions to time-space fractional Kuramoto-Sivashinsky model using the integrated Bäcklund transformation and Riccati-Bernoulli sub-ODE method. *AIMS Mathematics*. 2024; 9(5): 12357–12374. Available from: https://doi.org/10.3934/math.2024604.

[31] Al-Smadi M. Simplified iterative reproducing kernel method for handling time-fractional BVPs with error estimation. *Ain Shams Engineering Journal*. 2018; 9(4): 2517–2525. Available from: https://doi.org/10.1016/j.asej.2017.04.006.

[32] Momani S, Freihat A, Al-Smadi M. Analytical study of fractional-order multiple chaotic Fitzhugh-Nagumo neurons model using multistep generalized differential transform method. *Abstract and Applied Analysis*. 2014; 2024(1): 1–10. Available from: https://doi.org/10.1155/2014/276279.

[33] Al-Smadi M. Fractional residual series for conformable time-fractional Sawada–Kotera–Ito, Lax, and Kaup–Kupershmidt equations of seventh order. *Mathematical Methods in the Applied Sciences*. 2021. Available from: https://doi.org/10.1002/mma.6072.

[34] AL-Smadi MH, Gumah GN. On the homotopy analysis method for fractional SEIR epidemic model. *Research Journal of Applied Sciences, Engineering and Technology*. 2014; 7(18): 3809–3820. Available from: https://doi.org/10.19026/rjaset.7.738.

[35] Khalil H, Khan RA, H Al-Smadi M, A Freihat A. Approximation of solution of time fractional order three-dimensional heat conduction problems with Jacobi polynomials. *Punjab University Journal of Mathematics*. 2020; 47(1).

[36] Altawallbeh Z, Al-Smadi M, Abu-Gdairi R. Approximate solution of second-order integrodifferential equation of Volterra type in RKHS method. *International Journal of Mathematical Analysis*. 2013; 7(44): 2145–2160. Available from: http://dx.doi.org/10.12988/ijma.2013.36136.

[37] Oqielat MN, Eriqat T, Ogilat O, El-Ajou A, Alhazmi SE, Al-Omari S. Laplace-residual power series method for solving time-fractional reaction–diffusion model. *Fractal and Fractional*. 2023; 7(4): 309. Available from: https://doi.org/10.3390/fractalfract7040309.

[38] Alaroud M. Application of Laplace residual power series method for approximate solutions of fractional IVP's. *Alexandria Engineering Journal*. 2022; 61(2): 1585–1595. Available from: https://doi.org/10.1016/j.aej.2021.06.065.

[39] Alderremy AA, Shah R, Iqbal N, Aly S, Nonlaopon K. Fractional series solution construction for nonlinear fractional reaction-diffusion Brusselator model utilizing Laplace residual power series. *Symmetry*. 2022; 14(9): 1944. Available from: https://doi.org/10.3390/sym14091944.

[40] Sarhan A, Burqan A, Saadeh R, Al-Zhour Z. Analytical solutions of the nonlinear time-fractional coupled Boussinesq-Burger equations using Laplace residual power series technique. *Fractal and Fractional*. 2022; 6(11): 631. Available from: https://doi.org/10.3390/fractalfract6110631.

[41] Alquran M, Alsukhour M, Ali M, Jaradat I. Combination of Laplace transform and residual power series techniques to solve autonomous n-dimensional fractional nonlinear systems. *Nonlinear Engineering*. 2021; 10(1): 282–292. Available from: https://doi.org/10.1515/nleng-2021-0022.

[42] Shafee A, Alkhezi Y, Shah R. Efficient solution of fractional system partial differential equations using Laplace residual power series method. *Fractal and Fractional*. 2023; 7(6): 429. Available from: https://doi.org/10.3390/fractalfract7060429.